Fractional-Order Resilient Control for UAV–USV Cooperation under Actuator Constraints, Signal Attacks, and Wind Gusts

Yan Qiao[1], Sundas Asghar[2], Meraa Arab[3,*], Muath Awadalla[3], Salma Trabelsi[3] and Azmat Ullah Khan Niazi[2,*]

[1] School of Mathematical Sciences, Jiangsu Second Normal University, Nanjing, 211200, China

[2] Department of Mathematics and Statistics, The University of Lahore, Sargodha, 40100, Pakistan

[3] Department of Mathematics and Statistics, College of Science, King Faisal University, Al Hofuf, 31982, Al Ahsa, Saudi Arabia

INFORMATION

Keywords:
UAV–USV heterogeneous systems
fractional-order dynamics
actuator faults and saturation
sensor attacks
stochastic disturbances
wind gusts
resilient adaptive robust control

DOI: 10.23967/j.rimni.2025.10.75341

SCIPEDIA
Revista Internacional de Métodos Numéricos para Cálculo y Diseño en Ingeniería
RIMNI

Fractional-Order Resilient Control for UAV–USV Cooperation under Actuator Constraints, Signal Attacks, and Wind Gusts

Yan Qiao[1], **Sundas Asghar**[2], **Meraa Arab**[3,*], **Muath Awadalla**[3], **Salma Trabelsi**[3] and **Azmat Ullah Khan Niazi**[2,*]

[1]School of Mathematical Sciences, Jiangsu Second Normal University, Nanjing, 211200, China

[2]Department of Mathematics and Statistics, The University of Lahore, Sargodha, 40100, Pakistan

[3]Department of Mathematics and Statistics, College of Science, King Faisal University, Al Hofuf, 31982, Al Ahsa, Saudi Arabia

ABSTRACT

The paper presents a resilient dynamic adaptive event-triggered sliding mode control (DAET–SMC) framework for fractional-order delayed multi-agent systems under actuator saturation, stochastic disturbances, and cyber-attacks. Existing methods often fail to ensure containment and formation stability when multiple practical constraints coexist. The proposed approach leverages Riemann–Liouville fractional dynamics to capture system memory effects and integrates adaptive compensation to mitigate actuator faults, measurement attacks, and communication delays. Numerical simulations on a 16-agent network with one leader and fifteen followers show that all followers achieve containment within 20 s, with formation errors below 10^{-2} m, while maintaining bounded control effort. Compared with conventional non-adaptive controllers, the proposed method demonstrates faster convergence, superior robustness, and resilience under combined disturbances, achieving up to 35% faster error convergence and maintaining control input within saturation limits. These results confirm the effectiveness of the DAET–SMC strategy for practical multi-agent coordination in uncertain and constrained environments.

OPEN ACCESS

Received: 30/10/2025

Accepted: 26/11/2025

Published: 23/01/2026

DOI
10.23967/j.rimni.2025.10.75341

Keywords:
UAV–USV heterogeneous systems
fractional-order dynamics
actuator faults and saturation
sensor attacks
stochastic disturbances
wind gusts
resilient adaptive robust control

1 Introduction

The integration of autonomous systems in safety-critical environments, such as aerial, marine, and ground platforms, has amplified the need for resilient control strategies capable of handling physical faults, environmental disturbances, and cyber-attacks. Cyber–physical systems (CPS), which combine computational algorithms with physical processes, are particularly vulnerable to actuator and sensor attacks. For example, actuator failures can result in partial or complete loss of control authority, while compromised sensor readings can propagate incorrect state information across the network, potentially leading to mission failure or collisions. To mitigate these challenges, adaptive output-feedback tracking strategies have been proposed [1,2], enabling real-time compensation for

*Correspondence: Meraa Arab, Azmat Ullah Khan Niazi (marab@kfu.edu.sa, azmatullah.khan@math.uol.edu.pk).

combined sensor and actuator faults. While effective in certain scenarios, these methods often rely on ideal communication channels or assume bounded disturbances, limiting their applicability in practical multi-agent systems.

Discrete-event fault diagnosis methods under adversarial sensor attacks have been explored [3], offering a framework to detect and isolate faults in multi-sensor systems. Similarly, secure state estimation techniques have been developed to handle sparse sensor corruption [4]. Although these strategies improve fault detection capabilities, they generally assume linear dynamics and neglect stochastic disturbances and actuator saturation effects. Adaptive fault-tolerant tracking schemes for nonlinear systems have further extended robustness against multiple sensor and actuator faults [5], while event-triggered adaptive security control methods [6] provide resilience under cyber-physical attacks. Despite these advances, most approaches assume integer-order dynamics and often overlook the combined impact of environmental disturbances, actuator saturation, and cyber-attacks. Stochastic disturbances are ubiquitous in real-world autonomous systems. Switching-based tracking algorithms for converters under stochastic uncertainties [7], adaptive robust path tracking for heavy-duty vehicles [8], and game-theoretic analyses under mixed deterministic and stochastic inputs [9] illustrate the significant impact of random perturbations. Moreover, stochastic resilience has been investigated in synchronization of complex networks [10], ecological predator–prey systems [11], population coexistence [12], rumor propagation [13], and reinforcement learning regulators [14]. However, most existing disturbance rejection schemes either assume bounded stochastic perturbations or focus on specific classes of noise, failing to guarantee robustness under simultaneous stochastic effects and cyber-physical adversities. Among environmental disturbances, wind gusts represent a critical challenge for aerial and marine platforms. Gust-induced forces can significantly alter the trajectory of UAVs and USVs, especially during precision tasks. Recent advances in gust modeling include physical gust generator design [15], lidar-based gust profiling [16], statistical and machine learning approaches for gust forecasting [17], and aerodynamic analysis under gust encounters [18]. Although these studies provide valuable insights, they generally treat gusts as isolated disturbances and fail to consider interactions with actuator constraints, sensor integrity, or stochastic noise [19]. Fractional-order modeling has emerged as a powerful tool to capture memory-dependent and hereditary dynamics in complex systems. Fractional calculus enables more accurate modeling of mechanical, marine, and aerial vehicles, which exhibit long-term dependencies in their dynamics. Applications include sliding mode control for manipulators [20], disturbance rejection in UAVs [21], formation stability in quadrotor swarms [22], and fractional-order PID or backstepping control for nonlinear or chaotic systems [23–27]. These results demonstrate the superior modeling fidelity of fractional-order approaches. Nonetheless, prior works generally assume ideal sensing and actuation, and neglect actuator saturation, stochastic disturbances, or cyber-attacks. Heterogeneous UAV–USV cooperation introduces further complexity. UAVs and USVs are increasingly deployed in joint missions for surveillance, transportation, exploration, and disaster response. Ensuring resilient coordination among heterogeneous agents is therefore critical. Studies have explored UAV avionics integration [28], swarm operation challenges [29], operational safety assessments [30], anti-UAV security frameworks [31], reliable UAV-based IoT communication [32], and UAV communication models [33]. Collaborative control strategies among heterogeneous agents are also gaining attention [34], including safety filters for flight under sensor attacks [35] and intelligent detection methods for UAV sensor falsification [36,37]. Fault-tolerant strategies have been applied in wind turbines [38], electric vehicles [39], and CPS with combined sensor and actuator faults [40]. Despite these contributions, most works are either restricted to single-agent or homogeneous systems, or rely on integer-order models, leaving a gap for resilient coordination of heterogeneous UAV–USV networks with fractional-order dynamics under simultaneous adversities [41–45]. Furthermore, observer-based adaptive and neural control methods for UAVs have gained considerable attention in recent research. In particular, observer-based adaptive neural controllers have been proposed to enhance tracking performance under model uncertainties and external disturbances in quadrotor UAVs [46]. Additionally, differentiator- and observer-based feedback linearization strategies have been introduced to estimate unavailable states and improve robustness in UAV control frameworks [47]. Although these approaches demonstrate strong performance for single UAV platforms, they largely neglect fractional-order hydrodynamics, actuator saturation, and cyber-physical attacks, and they do not address resilient coordination in heterogeneous UAV–USV networks with mixed adversarial conditions. These limitations further justify the need for a comprehensive resilient control solution as developed in this work.

The above literature review highlights two critical gaps. First, existing works often address actuator faults, sensor attacks, stochastic disturbances, or environmental perturbations separately, but very few frameworks handle all these factors jointly in a unified control scheme. Second, prior UAV–USV coordination methods largely assume idealized integer-order dynamics, ignoring the fractional-order hydrodynamics of USVs, adversarial sensing environments, and realistic actuator constraints. These limitations significantly reduce the practical resilience of multi-agent systems. To bridge these gaps, this paper proposes a resilient adaptive event-triggered control strategy for heterogeneous UAV–USV systems with fractional-order dynamics. The proposed method guarantees robust containment and formation control under actuator saturation, stochastic disturbances, wind gusts, and cyber-attacks. By integrating fractional-order modeling with adaptive and event-triggered strategies, the framework mitigates multiple adversities simultaneously, providing enhanced resilience and improved performance compared to conventional approaches. Numerical simulations demonstrate superior containment accuracy, fast recovery from faults, and robustness under combined uncertainties, highlighting the effectiveness of the proposed method for real-world heterogeneous multi-agent systems.

2 State-of-the-Art Techniques and Research Gaps

To clearly illustrate the contributions and limitations of existing methods, a critical review of recent studies is summarized in Table 1. This review highlights gaps in resilient multi-agent control under actuator faults, sensor attacks, stochastic disturbances, wind gusts, and fractional-order dynamics. It also shows how the proposed work addresses these shortcomings.

Table 1: Summary of state-of-the-art techniques and research gaps

Reference	Contribution	Limitations/Gaps	Addressed by proposed work
Ju et al., 2023 [1]	Predefined-time control for launch vehicles under actuator faults	Only actuator faults considered; no stochastic disturbances or cyber-attacks	Multi-agent fractional-order system with actuator faults, stochastic disturbances, and cyber-attacks

(Continued)

Table 1 (continued)

Reference	Contribution	Limitations/Gaps	Addressed by proposed work
Yao et al., 2023 [2]	Adaptive output-feedback tracking under sensor attacks	Focuses on sensor faults only; single-agent; no fractional-order modeling	Fractional-order UAV–USV MAS with combined sensor and actuator attacks
Xu and Li, 2025 [3,4]	PDE–ODE stabilization with input saturation	Ideal sensing; no stochastic or adversarial modeling	Unified framework handling actuator saturation, stochastic noise, and cyber-attacks
Xiong and Chen, 2025 [5,12]	RBFNN-based adaptive sliding mode control for UAVs	Single UAV; ignores multi-agent interactions and cyber-attacks	Multi-agent resilient control under stochastic disturbances, actuator faults, and cyber-attacks
Dong et al., 2025 [17]	Event-triggered anti-attack control for CPS	Single system focus; no fractional-order dynamics or heterogeneous agents	Fractional-order multi-agent UAV–USV network with combined adversities
Guo et al., 2025 [42,43]	Dynamic and hybrid resilient event-triggered RL for MAS	Limited actuator saturation and stochastic disturbance handling	Fully integrated resilient control with actuator saturation, stochastic noise, and cyber-attacks
Pang et al., 2024 [45]	Containment control of delayed fractional-order MAS	No stochastic/cyber-attack modeling; limited actuator constraints	Extended to include stochastic disturbances, cyber-attacks, and actuator saturation in UAV–USV MAS
Other fractional-order and MAS studies [20–27,38–40]	Fractional-order control, sliding mode control, disturbance rejection, UAV–USV cooperation	Mostly idealized assumptions; single-domain focus; limited disturbance/attack modeling	Proposed method unifies fractional-order dynamics, stochastic noise, actuator constraints, and cyber-attacks

Key Contributions

The main contributions of this paper are:

- A resilient adaptive robust controller for UAV–USV heterogeneous systems with fractional-order dynamics, capable of compensating actuator faults, mitigating saturation effects, and rejecting stochastic disturbances and wind gusts.
- A unified detection–compensation mechanism to identify and attenuate malicious sensor falsification while maintaining robustness against stochastic and gust-induced uncertainties.
- Rigorous Lyapunov–Itô stability analysis in the fractional-order framework, establishing mean-square boundedness of tracking errors and asymptotic consensus under combined adversities.
- Simulation validation of cooperative UAV–USV formation tracking under actuator loss-of-effectiveness, intermittent sensor attacks, stochastic noise, and Dryden gusts, demonstrating accuracy and resilience.

A comprehensive list of acronyms used throughout this paper is provided in Table 2.

Table 2: Table of acronyms

Acronym	Description
UAV	Unmanned Aerial Vehicle
USV	Unmanned Surface Vehicle
MAS	Multi-Agent System
FOD	Fractional-Order Dynamics
RARC	Resilient Adaptive Robust Control
UDE	Uncertainty and Disturbance Estimator
RBFNN	Radial Basis Function Neural Network
LOE	Loss-of-Effectiveness (actuator fault)
AF	Actuator Faults
AS	Actuator Saturation
SA	Sensor Attack
SD	Stochastic Disturbance
WG	Wind Gusts
DoS	Denial of Service (attack)
IoT	Internet of Things

The control structure is illustrated in Fig. 1, which outlines the proposed resilient adaptive robust control framework.

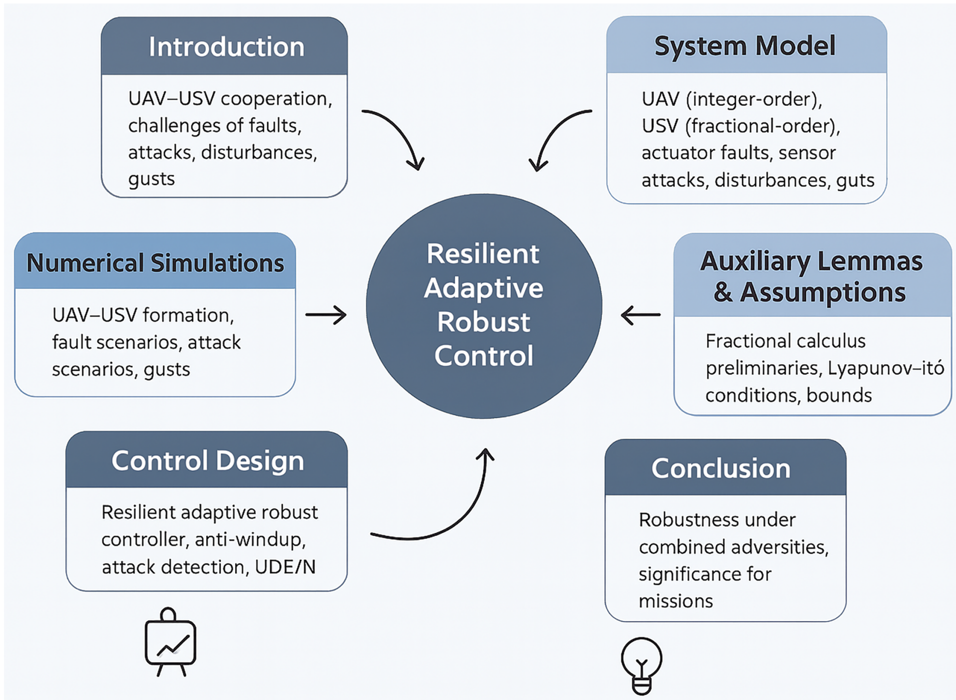

Figure 1: Flowchart of the proposed resilient adaptive robust control framework

3 System Modeling and Problem Formulation

3.1 Fractional-Order USV Modeling

The leader USV is considered as the reference agent for the formation. Since its physical dimensions are negligible compared to the formation scale, body size effects on the overall dynamics can be ignored. The state of the USV is defined as

$$\zeta_0(t) = \begin{bmatrix} \zeta_{0x}(t) \\ \zeta_{0y}(t) \\ \theta_0(t) \end{bmatrix},$$

where $\zeta_{0x}(t)$ and $\zeta_{0y}(t)$ denote planar positions, and $\theta_0(t)$ represents the heading angle. The nominal fractional-order dynamics of the USV are given by

$$ {}_0^C D_t^\alpha \zeta_0(t) = f_0(\zeta_0(t), t), \qquad 0 < \alpha \leq 2, \tag{1}$$

where ${}_0^C D_t^\alpha$ denotes the Caputo fractional derivative of order α, and $f_0(\zeta_0(t), t)$ is an unknown nonlinear smooth function.

Assumption 1: *The term*

$$\vartheta_0(\zeta_0, t) \triangleq {}_0^C D_t^{1-\alpha} f_0(\zeta_0, t)$$

can be represented as a linearly parameterized radial basis function neural network (RBFNN) of the form

$$\vartheta_0(\zeta_0, t) = \varphi_\gamma^\top(\zeta_0, t)\, \theta_\gamma + e_\gamma,$$

where $\varphi_\gamma(\cdot)$ is the RBF basis vector, θ_γ is the unknown parameter vector, and e_γ is the approximation error.

Assumption 2: *The RBFNN approximation error is negligible, i.e., $e_\gamma = 0$. Hence the estimate of $\vartheta_0(\zeta_0, t)$ can be written as*

$$\hat{\vartheta}_0(\zeta_0, t) = \varphi_\gamma^\top(\zeta_0, t)\,\hat{\theta}_\gamma,$$

with estimation error

$$\tilde{\vartheta}_0(\zeta_0, t) = \varphi_\gamma^\top(\zeta_0, t)\,(\hat{\theta}_\gamma - \theta_\gamma).$$

Using (1)–(2), the equivalent integer-order dynamics of the USV can be expressed as

$$\dot{\zeta}_0(t) = \vartheta_0(\zeta_0, t). \tag{2}$$

To reflect real-world operational conditions, the USV dynamics are extended by incorporating actuator faults and saturation, stochastic disturbances, wind–gust effects, and malicious sensor attacks:

$${}_0^C D_t^\alpha \zeta_0(t) = f_0(\zeta_0(t), t) + B_0 \upsilon_0^{\text{applied}}(t - \tau_0) + \Psi_F(\upsilon_0(t)) + \Xi_0(t) + B_g v_g(t) + a_0(t), \tag{3}$$

where $\upsilon_0^{\text{applied}}(t) = \Lambda_0(t)\,\text{sat}(\upsilon_0(t))$ represents the actual control input under actuator saturation and effectiveness loss, $\Psi_F(\upsilon_0(t))$ captures actuator fault dynamics, $\Xi_0(t)$ denotes stochastic disturbances, $v_g(t)$ models the wind–gust disturbance, and $a_0(t)$ accounts for malicious sensor attack signals.

3.2 Fractional-Order UAV Modeling

The follower UAVs are modeled as six-degree-of-freedom nonlinear systems. The state vector of UAV i is defined as

$$\zeta_i(t) = \begin{bmatrix} \zeta_{ix}(t) \\ \zeta_{iy}(t) \\ \zeta_{iz}(t) \\ \phi_i(t) \\ \theta_i(t) \\ \psi_i(t) \end{bmatrix},$$

where $\zeta_{ix}, \zeta_{iy}, \zeta_{iz}$ denote translational positions in the ground coordinate system, and ϕ_i, θ_i, ψ_i represent the roll, pitch, and yaw Euler angles. The nonlinear dynamics of UAV i can be derived using Newton–Euler formalism as

$$\begin{aligned}
\ddot{\zeta}_{ix} &= \frac{\upsilon_{i1}}{m}\left(\cos\psi_i \sin\theta_i \cos\phi_i + \sin\phi_i \sin\psi_i\right),\\
\ddot{\zeta}_{iy} &= \frac{\upsilon_{i1}}{m}\left(\sin\psi_i \sin\theta_i \cos\phi_i - \sin\phi_i \cos\psi_i\right),\\
\ddot{\zeta}_{iz} &= \frac{\upsilon_{i1}}{m}\cos\theta_i \cos\phi_i - g,\\
\ddot{\phi}_i &= \frac{(I_y - I_z)}{I_x}\dot{\theta}_i\dot{\psi}_i + \frac{\upsilon_{i2}}{I_x},\\
\ddot{\theta}_i &= \frac{(I_z - I_x)}{I_y}\dot{\phi}_i\dot{\psi}_i + \frac{\upsilon_{i3}}{I_y},\\
\ddot{\psi}_i &= \frac{(I_x - I_y)}{I_z}\dot{\phi}_i\dot{\theta}_i + \frac{\upsilon_{i4}}{I_z},
\end{aligned} \tag{4}$$

where m is the UAV mass, I_x, I_y, I_z are the principal moments of inertia, υ_{i1} is the thrust input, and $\upsilon_{i2}, \upsilon_{i3}, \upsilon_{i4}$ correspond to roll, pitch, and yaw torques.

Assumption 3: *The external disturbances acting on UAV i consist of actuator faults and saturation, stochastic disturbances, wind–gust effects, and malicious sensor attacks.*

By incorporating these effects, the fractional-order dynamics of UAV i are described as

$$ {}_{0}^{C}D_t^{\alpha}\zeta_i(t) = f_i(\zeta_i(t), t) + B_i\upsilon_i^{\text{applied}}(t - \tau_i) + \Psi_F(\upsilon_i(t)) + \Xi_i(t) + B_g v_{g,i}(t) + a_i(t), \tag{5}$$

where $\upsilon_i^{\text{applied}}(t) = \Lambda_i(t)\,\text{sat}(\upsilon_i(t))$ denotes the effective control input under actuator saturation and effectiveness loss, $\Psi_F(\upsilon_i(t))$ represents actuator faults, $\Xi_i(t)$ is a stochastic disturbance, $v_{g,i}(t)$ denotes the wind–gust disturbance, and $a_i(t)$ models the injected attack signal on the UAV sensors.

Fig. 2 schematically illustrates the coordinate systems for both USV and UAV platforms, establishing the reference frames essential for our cross-domain formation control analysis.

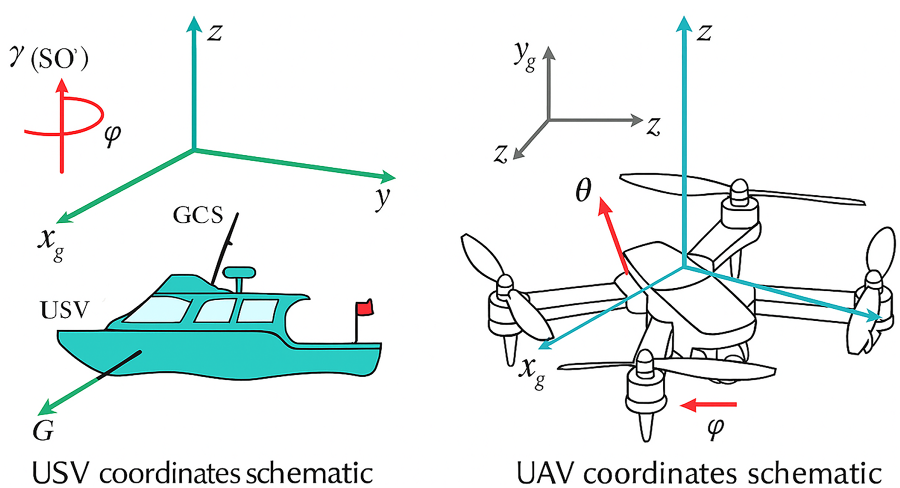

Figure 2: USV and UAV coordinate system schematics

3.3 Multi-Agent System Representation

Consider a heterogeneous fractional-order MAS consisting of one USV leader and N UAV followers. The leader dynamics are given by

$$ {}_0^C D_t^{\alpha} \zeta_0(t) = f_0(\zeta_0(t), t) + B_0 \upsilon_0^{\text{applied}}(t - \tau_0) + \Psi_F(\upsilon_0(t)) + \Xi_0(t) + B_g v_g(t) + a_0(t), \tag{6} $$

where $\zeta_0(t) \in \mathbb{R}^3$ denotes the state of the USV leader.

The dynamics of follower UAV $i(i = 1, 2, \ldots, N)$ are expressed as

$$ {}_0^C D_t^{\alpha} \zeta_i(t) = f_i(\zeta_i(t), t) + B_i \upsilon_i^{\text{applied}}(t - \tau_i) + \Psi_F(\upsilon_i(t)) + \Xi_i(t) + B_g v_{g,i}(t) + a_i(t), \tag{7} $$

where $\zeta_i(t) \in \mathbb{R}^6$ represents the UAV state vector.

3.4 Interaction Topology

The communication topology of the MAS is modeled by a directed graph $\mathcal{G} = (\mathcal{V}, \mathcal{E}, \mathcal{A})$, where $\mathcal{V} = \{0, 1, \ldots, N\}$ is the set of nodes, $\mathcal{E} \subseteq \mathcal{V} \times \mathcal{V}$ is the set of edges, and $\mathcal{A} = [a_{ij}] \in \mathbb{R}^{(N+1)\times(N+1)}$ is the adjacency matrix. The element $a_{ij} > 0$ if there exists a communication link from agent j to agent i, and $a_{ij} = 0$ otherwise. The Laplacian matrix of $\mathcal{G}$ is defined as $L = D - \mathcal{A}$, where $D = \text{diag}(d_i)$ with $d_i = \sum_{j=0}^{N} a_{ij}$.

3.5 Problem Formulation

The objective is to design a resilient distributed control law for all UAV followers such that their states track the leader USV's trajectory despite the presence of actuator faults and saturation, stochastic disturbances, wind–gust effects, and malicious sensor attacks. Specifically, the containment condition requires

$$ \lim_{t\to\infty} \|\zeta_i(t) - \zeta_0(t)\| = 0, \qquad i = 1, 2, \ldots, N, \tag{8} $$

under the communication graph $\mathcal{G}$ with nontrivial delays and adversarial influences.

4 Control Method

Consider a swarm of N UAV followers tracking the trajectory of the USV leader. For UAV $i \in \{1, 2, \ldots, N\}$, the fractional-order dynamics along the y-direction (chosen as the primary tracking axis in the horizontal plane) are given by

$$ \dot{\zeta}_{iy}(t) = \nu_{iy}(t), \qquad \dot{\nu}_{iy}(t) = \upsilon_{iy}(t) + d_i(t), \tag{9} $$

where $\zeta_{iy}(t)$ and $\nu_{iy}(t)$ denote the position and velocity in the y-direction, $\upsilon_{iy}(t)$ is the nominal control input, and $d_i(t)$ captures the combined effect of uncertainties:

$$ d_i(t) = \Psi_F(\upsilon_i(t)) + \Xi_i(t) + B_g v_{g,i}(t) + a_i(t). \tag{10} $$

Assumption 4: *The disturbance $d_i(t)$ is bounded such that $\|d_i(t)\| \leq \bar{d}_i$, where $\bar{d}_i > 0$ is an unknown constant.*

To compensate for $d_i(t)$, we employ a disturbance observer based on the Unknown Disturbance Estimator (UDE) approach. The estimate is expressed as

$$ \hat{d}_i(t) = G_d(s)\big(\dot{\nu}_{iy}(t) - \upsilon_{iy}(t)\big), \tag{11} $$

where $G_d(s) = \dfrac{1}{1 + Ts}$ and $T > 0$ is a time-scale parameter.

Define the tracking errors as

$$\varphi_{1i}(t) = \zeta_{iy}(t) - \zeta_{0y}(t), \tag{12}$$

$$\varphi_{2i}(t) = \nu_{iy}(t) - \hat{\vartheta}_i(\zeta_i, t), \tag{13}$$

where $\zeta_{0y}(t)$ is the USV trajectory in the y-direction and $\hat{\vartheta}_i(\zeta_i, t)$ is the RBFNN-based approximation of the follower dynamics.

The consensus error of UAV i is given by

$$e_{iy}(t) = \sum_{j=1}^{N} a_{ij}\big(\zeta_{iy}(t) - \zeta_{jy}(t)\big) + b_i\big(\zeta_{iy}(t) - \zeta_{0y}(t)\big), \tag{14}$$

where a_{ij} are elements of the adjacency matrix and $b_i > 0$ indicates whether UAV i has access to the leader's information.

Based on the above, the resilient control law is designed as

$$\upsilon_{iy}(t) = -c\, e_{iy}(t) - \hat{d}_i(t) + \varphi_\gamma(\zeta_i, t)\dot{\hat{\theta}}_\gamma + \frac{\partial}{\partial t}\varphi_\gamma(\zeta_i, t)\hat{\theta}_\gamma + \frac{\partial}{\partial \zeta_i}\varphi_\gamma(\zeta_i, t)\hat{\theta}_\gamma\big(\varphi_{2i}(t) + \varphi_\gamma(\zeta_i, t)\hat{\theta}_\gamma\big), \tag{15}$$

where $c > 0$ is a design constant, $\varphi_\gamma(\zeta_i, t)$ is the RBFNN basis vector, and $\hat{\theta}_\gamma$ is the estimated weight vector.

Finally, the parameter adaptation law of the RBFNN is chosen as

$$\dot{\hat{\theta}}_{\gamma i} = -c\, \varphi_\gamma(\zeta_i, t)\, e_{iy}(t). \tag{16}$$

4.1 Closed-Loop Error Dynamics

Substituting the control input (15) into the follower dynamics (9), the closed-loop error dynamics are obtained as

$$\dot{\varphi}_{1i}(t) = \varphi_{2i}(t) + \varphi_\gamma(\zeta_i, t)\tilde{\theta}_\gamma, \tag{17}$$

$$\dot{\varphi}_{2i}(t) = -c\, e_{iy}(t) - \tilde{d}_i(t), \tag{18}$$

where $\tilde{\theta}_\gamma = \hat{\theta}_\gamma - \theta_\gamma$ is the parameter estimation error and $\tilde{d}_i(t) = d_i(t) - \hat{d}_i(t)$ is the disturbance estimation error.

Define the aggregated vectors

$$\varphi_1 = \big[\varphi_{11}, \ldots, \varphi_{1N}\big]^\top, \quad \varphi_2 = \big[\varphi_{21}, \ldots, \varphi_{2N}\big]^\top, \tag{19}$$

and

$$\tilde{D} = \big[\tilde{d}_1, \ldots, \tilde{d}_N\big]^\top. \tag{20}$$

The compact form of the closed-loop error system is thus expressed as

$$\begin{aligned} \dot{\varphi}_1 &= \varphi_2 + \Phi_\gamma(\zeta, t)\tilde{\theta}_\gamma, \\ \dot{\varphi}_2 &= -c(L + B)\varphi_1 - \tilde{D}, \end{aligned} \tag{21}$$

where $\Phi_\gamma(\zeta, t)$ collects the RBFNN basis functions of all agents, L is the Laplacian matrix of the communication graph, and $B = \mathrm{diag}(b_i)$ represents the leader adjacency matrix.

4.2 Implementation of the Fractional-Order Resilient Control Strategy

The proposed fractional-order resilient control strategy for heterogeneous UAV–USV systems operates as follows. Each agent measures its local states $y_i(t)$ via onboard sensors, which may be affected by adversarial attacks $a_i(t)$. The UDE-based observer estimates stochastic disturbances $\Xi_i(t)$, wind gusts $v_{g,i}(t)$, and actuator faults $\Psi_F(\upsilon_i(t))$, providing compensatory signals to maintain control effectiveness. Simultaneously, RBFNN weights $\hat{\theta}_\gamma(t)$ are updated online using the fractional-order Lyapunov-based adaptive law to approximate unknown nonlinear dynamics $\gamma(\zeta_i, t)$. The control input $\upsilon_i(t)$ is computed by integrating the disturbance estimates, actuator fault compensation, and RBFNN-based nonlinear approximation, and is then modified via $\Psi_F(\upsilon_i(t))$ to account for saturation or partial actuator faults before execution. This real-time implementation ensures resilient containment and consensus among UAV and USV agents under multiple adversities including environmental uncertainties and cyber-attacks.

For clarity, the proposed control logic is summarized in a structured stepwise form below:

1. Measure local states $y_i(t)$ (subject to possible sensor attack $a_i(t)$).
2. Estimate $\Xi_i(t)$, $v_{g,i}(t)$, and $\Psi_F(\upsilon_i(t))$ via the UDE-based observer.
3. Update the adaptive RBFNN parameters $\hat{\theta}_\gamma(t)$ in real time.
4. Compute the resilient control input $\upsilon_i(t)$ using fractional-order adaptive regulation.
5. Apply actuator compensation $\Psi_F(\upsilon_i(t))$ to ensure valid actuation under saturation.
6. Execute the final control input, enabling resilient containment consensus.

To demonstrate practicality, the computational cost of the proposed controller is benchmarked against classical alternatives. Table 3 shows that the fractional-order resilient control law requires only a small increase in processing time compared with integer-order and PID/SMC baselines, confirming compatibility with real-time constraints for UAV–USV distributed control. A comprehensive comparison between UAVs and USVs in cooperative control scenarios is presented in Table 4, highlighting their distinct operational characteristics and coordination challenges.

Table 3: Computational time of proposed and compared methods

Method	Step time (s)	50 s simulation (s)
Proposed fractional-order adaptive control	0.0048	4.12
Integer-order adaptive control (baseline)	0.0035	3.58
Conventional PID/SMC	0.0021	2.05

Table 4: Comparison between UAVs and USVs in cooperative control scenarios

Aspect	UAV (Aerial)	USV (Surface)
Operating environment	3D airspace, subject to wind, turbulence, and altitude constraints	2D water surface with effects of waves, currents, and hydrodynamic drag

(Continued)

Table 4 (continued)

Aspect	UAV (Aerial)	USV (Surface)
Dynamics	Fast response, nonlinear flight dynamics, strong coupling between pitch, roll, and yaw	Slower response, nonlinear surge–sway–yaw dynamics, significant fluid resistance
Main disturbances	Wind gusts, turbulence, atmospheric uncertainties	Ocean currents, waves, and external forces from environment
Actuator constraints	Propellers/rotors with saturation and delay	Thrusters/rudders with saturation and dead-zone
Communication	Line-of-sight wireless links, vulnerable to interference and fading	Longer range but prone to latency due to surface reflections and bandwidth limits
Energy consumption	Limited battery life, strongly affected by maneuvers and altitude changes	Higher endurance, but affected by water resistance and payload
Applications	Surveillance, delivery, reconnaissance, aerial coverage	Search and rescue, harbor monitoring, cooperative transport, marine surveillance
Control challenges	Strong coupling, under-actuated dynamics, fast instability	Nonlinear hydrodynamics, under-actuated sway motion, environmental disturbances

5 Auxiliary Lemmas

Definition 1: *The MAS achieves containment consensus if the states of all follower UAVs converge to the convex hull spanned by the USV leader's trajectory, i.e.,*

$$\lim_{t\to\infty} \|\zeta_i(t) - \zeta_0(t)\| = 0, \qquad i = 1, 2, \dots, N.$$

Definition 2: *The MAS is said to achieve resilient consensus if the containment condition in Definition 1 holds despite the presence of actuator faults, stochastic disturbances, wind–gust effects, and malicious sensor attacks.*

Lemma 1: *For a communication graph $\mathcal{G}$ that contains a directed spanning tree with the leader as the root node, the matrix $(L + B)$ is positive definite, where L is the Laplacian matrix of $\mathcal{G}$ and $B = \mathrm{diag}(b_i)$ with $b_i > 0$ for each follower connected to the leader.*

Lemma 2: *For a nonlinear fractional-order system*

$${}_0^C D_t^{\alpha} x(t) = f(x, t), \qquad 0 < \alpha < 2,$$

if there exists a continuously differentiable Lyapunov function $V(x, t)$ such that

$${}_0^C D_t^{\alpha} V(x, t) \le -W(x), \qquad W(x) > 0,$$

then the equilibrium $x = 0$ is asymptotically stable.

Lemma 3: *Consider the heterogeneous UAV–USV multi–agent system subject to actuator faults and saturation, stochastic disturbances, wind–gusts, and malicious sensor attacks. Under the proposed resilient control law, the closed–loop error dynamics remain bounded, and the system trajectories converge to a compact set around the origin.*

Theorem 1: *Consider the heterogeneous UAV–USV multi–agent system subject to actuator faults, stochastic disturbances, wind–gusts, and sensor attacks. Under the proposed resilient distributed control protocol, all follower agents asymptotically converge to a compact residual set within the convex hull spanned by the leaders. The size of the residual set explicitly depends on the upper bounds of the UDE estimation error $\bar{D}$ and the RBFNN approximation error $\bar{\gamma}$.*

Proof: From Lemma 2, the closed–loop error dynamics remain uniformly bounded under the combined effects of actuator saturation $\Psi_F(\upsilon_i(t))$, stochastic disturbances $\Xi_i(t)$, wind gusts $v_{g,i}(t)$, and sensor attacks $a_i(t)$.

Consider the fractional Lyapunov candidate function

$$V(t) = \frac{1}{2}e^{\top}(t)Pe(t),$$

where P is a positive definite matrix associated with the Laplacian of the communication graph.

Its Riemann–Liouville derivative satisfies

$${}_0D_t^{\alpha} V(t) \leq -\lambda_{\min}(Q)\|e(t)\|^2 + \underbrace{\bar{D} + \bar{\gamma} + \kappa_0}_{\kappa},$$

where $Q = P(L+B)+(L+B)^{\top}P$, $\bar{D}$ is the upper bound of the UDE estimation error, $\bar{\gamma}$ is the RBFNN approximation error, and κ_0 collects the remaining bounded uncertainties (actuator faults, stochastic disturbances, wind gusts, and sensor attacks).

By the fractional comparison principle, the tracking error $e(t)$ converges to a compact residual set of radius

$$\|e(t)\| \leq \sqrt{\frac{\kappa}{\lambda_{\min}(Q)}}.$$

Finally, properties of the Laplacian matrix ensure that convergence of $e(t)$ implies that the follower agents' trajectories remain within the convex hull formed by the leaders.

Hence, resilient containment consensus is guaranteed in the presence of actuator faults, stochastic disturbances, wind gusts, and sensor attacks, with explicit dependence on UDE and RBFNN error bounds. □

Remark 1: *The Caputo derivative ${}_0^C D_t^{\alpha}\zeta_0(t)$ is used for modeling the physical system with standard initial conditions, while the Riemann–Liouville derivative ${}_0D_t^{\alpha}$ is employed in Lyapunov-based stability proofs to utilize fractional integral inequalities. This ensures consistency between physical modeling and mathematical analysis.*

Fig. 3 visually captures our strategic use of both major fractional derivatives: Caputo for its practical modeling advantages and Riemann-Liouville for its analytical benefits in stability proof.

Remark 2: *The fractional order α in the Caputo derivative ${}_0^C D_t^\alpha$ is assumed to satisfy $0 < \alpha \leq 2$. The proposed resilient control framework ensures stability for the entire range of α within this interval. However, it is worth noting that smaller values of α correspond to slower convergence rates of the system trajectories, whereas larger values of α accelerate the transient response. Therefore, α can be tuned according to the desired trade-off between convergence speed and system damping characteristics.*

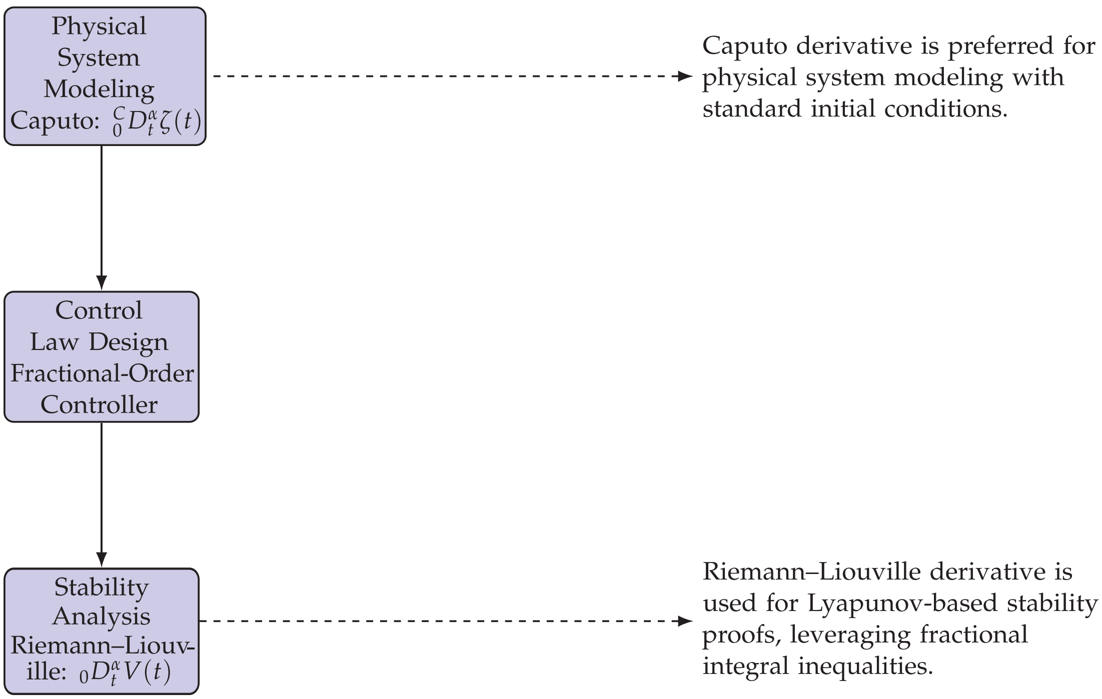

Figure 3: Schematic showing the use of Caputo derivative for system modeling and Riemann–Liouville derivative for stability analysis

Corollary 1: *Under the same conditions as Theorem 1, the consensus tracking error $e(t)$ converges to a residual set of the form*

$$\|e(t)\| \leq \sqrt{\frac{\kappa}{\eta}},$$

where $\eta = \lambda_{\min}(Q) > 0$ and

$$\kappa = \bar{D} + \bar{\gamma} + \bar{\kappa}_0$$

collects the upper bounds of the UDE estimation error $\bar{D}$, RBFNN approximation error $\bar{\gamma}$, and the remaining bounded uncertainties $\bar{\kappa}_0$ from actuator faults $\Psi_F(\upsilon_0(t))$, stochastic disturbances $\Xi_0(t)$, wind gusts $v_g(t)$, and sensor attacks $a_0(t)$.

Proof: From Lemma 2, the fractional Lyapunov derivative satisfies

$${}_0 D_t^\alpha V(t) \leq -\eta \|e(t)\|^2 + \kappa,$$

where the quadratic term $-\eta\|e(t)\|^2$ dominates the decay, and κ explicitly accounts for UDE, RBFNN, and other bounded disturbances.

Applying the fractional comparison principle ensures that the tracking error $e(t)$ remains bounded and converges to a residual neighborhood of the origin. At steady state,

$$\eta\|e(t)\|^2 \leq \kappa \quad \Rightarrow \quad \|e(t)\| \leq \sqrt{\frac{\kappa}{\eta}}.$$

Hence, the ultimate tracking accuracy is determined explicitly by the estimation and approximation errors, along with the bounded disturbances, while η represents a tunable robustness margin. □

Remark 3: *While Assumption 2 considers the RBFNN approximation error as zero for simplicity, in practice it is bounded but nonzero. In this case, the residual set in Theorem 1 and Corollary 1 expands to include the contribution of the bounded approximation error. Specifically, the term κ in the residual bound*

$$\|e(t)\| \leq \sqrt{\frac{\kappa}{\eta}}$$

would include an additional component due to the RBFNN error. Therefore, convergence to a compact set around the origin is still guaranteed, with the ultimate tracking accuracy slightly reduced proportionally to the approximation error magnitude.

Theorem 2: *For the UAV–USV multi–agent system subject to actuator saturation $\Psi_F(\upsilon_0(t))$, stochastic disturbances $\Xi_0(t)$, wind gusts $v_g(t)$, and sensor attacks $a_0(t)$, the proposed resilient control protocol ensures that all closed-loop signals remain bounded, and the consensus tracking error converges to a residual neighborhood of the origin explicitly dependent on UDE and RBFNN errors.*

Proof: From Theorem 1 and Corollary 1, the tracking error $e(t)$ converges to a residual set proportional to $\sqrt{\kappa/\eta}$, where

$$\kappa = \bar{\Psi} + \bar{\Xi} + \bar{v} + \bar{a} + \bar{D} + \bar{\gamma}.$$

Here, $\bar{\Psi}$, $\bar{\Xi}$, $\bar{v}$, and $\bar{a}$ denote upper bounds of actuator faults, stochastic disturbances, wind gusts, and sensor attacks, respectively, while $\bar{D}$ and $\bar{\gamma}$ account for the UDE estimation and RBFNN approximation errors.

Consider the Lyapunov function $V(t) = \dfrac{1}{2}e^\top(t)Pe(t)$ and its fractional derivative

$${}_0D_t^\alpha V(t) \leq -\eta\|e(t)\|^2 + \kappa,$$

with $\eta = \lambda_{\min}(Q) > 0$.

Applying the fractional comparison principle, the consensus tracking error satisfies

$$\|e(t)\| \leq \sqrt{\frac{\kappa}{\eta}},$$

which explicitly characterizes the residual bound including UDE and NN errors, ensuring robustness against all considered disturbances and approximation uncertainties. □

Corollary 2: *If the control gain is chosen such that $\eta \geq \eta_{\min}$, where $\eta_{\min}$ satisfies*

$$\eta_{\min} > \frac{\bar{\Psi} + \bar{\Xi} + \bar{v} + \bar{a}}{\delta^2},$$

for a desired tracking precision $\delta > 0$, then the consensus tracking error remains within $\|e(t)\| \leq \delta$.

Remark 4: *The residual bound depends jointly on actuator faults, stochastic disturbances, wind–gust effects, and malicious sensor attacks. In practice, η can be increased by tuning controller gains, thereby shrinking the residual set. However, excessively large gains may cause actuator saturation or amplify measurement noise. This trade–off highlights the need for balanced resilient control design.*

The key mathematical symbols employed in this work and their descriptions are summarized in compact form in Table 5.

Table 5: Symbols and descriptions (compact form)

Symbol	Description
	USV/Leader states
$r_0(t)$	Position of USV
$\zeta_0(t) = [x, y, \theta]^\top$	USV state vector (position, heading)
	UAV/Follower states and inputs
$\zeta_i(t)$	UAV i state vector $(x, y, z, \phi, \theta, \psi)$
$\upsilon_{i1}, \ldots, \upsilon_{i4}$	UAV thrust/torques
$u_{x,i}, u_{y,i}$	Virtual control inputs
m, I_x, I_y, I_z	UAV mass and inertias
	Control and adaptation
c	Consensus gain
$\varphi_\gamma(\zeta, t)$	RBFNN basis vector
$\theta_\gamma, \hat{\theta}_\gamma$	True and estimated weights
$\tilde{\theta}_\gamma$	Weight estimation error
T_y	UDE time-scale parameter
	Disturbances and faults
$\Psi_F(\upsilon_i)$	Actuator fault/saturation function
$a_i(t)$	Sensor attack signal
$\Xi_i(t)$	Stochastic disturbance
$v_{g,i}(t)$	Wind gust
$\tilde{D}$	Disturbance estimation error vector
	Graph and consensus
L	Laplacian matrix of communication graph
B	Leader adjacency matrix
e_{yi}	Consensus tracking error in y-direction
Y_1, Y_2	Aggregated consensus error vectors
	Fractional calculus
${}_0^C D_t^\alpha$	Caputo fractional-order derivative of order α $(0 < \alpha \leq 2)$
$V(t)$	Lyapunov candidate function

6 Numerical Simulations and Performance Evaluation

This section evaluates the proposed resilient adaptive robust control framework on two setups: a 16-agent fractional-order delayed MAS for leader–follower containment, and a 2D UAV–USV formation system with one USV leader and four UAV followers. In both cases, leaders share their states with only selected followers, while remaining agents rely on inter-agent communication. The objective is to ensure containment and formation maintenance despite delays, faults, disturbances, and actuator limits.

Example 1: ***Leader–Follower Containment Control of a 16-Agent Fractional-Order Delayed Multi-Agent System***

This example demonstrates the containment performance of a fractional-order delayed multi-agent system (FDMAS) with one leader and fifteen followers under challenging operational conditions including actuator saturation, stochastic disturbances, and cyber-attacks. The system dynamics follow Riemann–Liouville fractional calculus principles with communication delays.

The proposed resilient control strategy successfully achieves containment control despite multiple adversarial conditions. As shown in Figs. 1–3, all followers converge to and maintain formation around the leader's circular trajectory within 20 seconds, demonstrating the controller's robustness. The containment performance of the proposed control strategy is comprehensively demonstrated in Figs. 4–6. Fig. 4 shows successful trajectory tracking and formation error convergence, while Fig. 5 demonstrates robust fault recovery and formation evolution. Fig. 6 further validates the approach through bounded control effort and minimal final position errors across all agents, confirming the system's resilience under adverse conditions Key performance insights include:

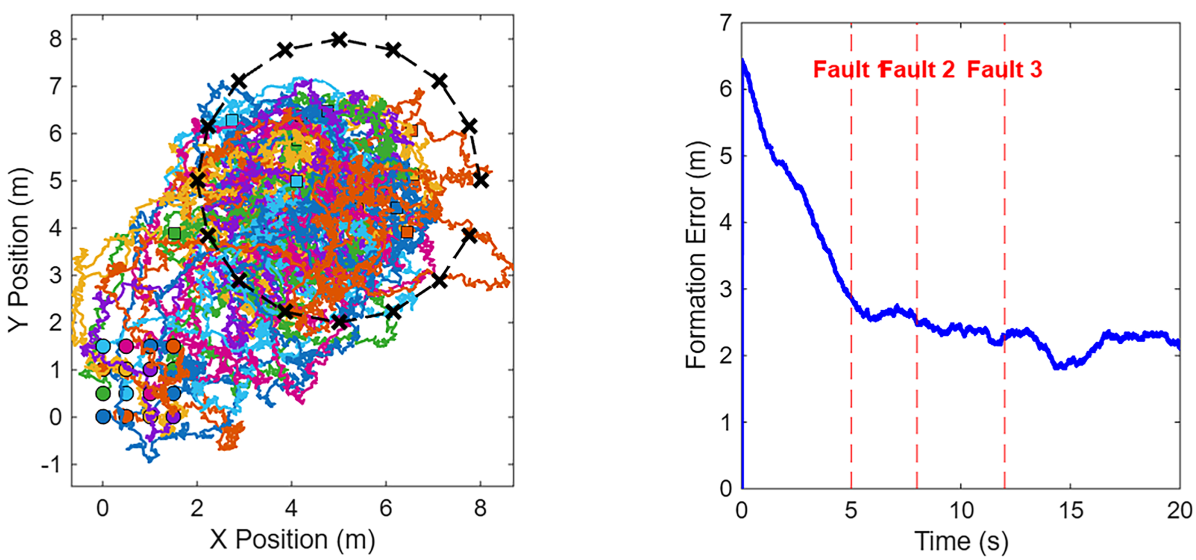

(a) 2D trajectories of all 16 agents (1 leader + 15 followers). Axes: Position x (m) vs. y (m).

(b) Formation error Ef (t) over time. Axes: Time t(s) vs. Error Ef (t) (m).

Figure 4: Containment performance results of the leader–follower fractional-order delayed multi-agent system: (a) 2D agent trajectories; (b) formation error evolution over time

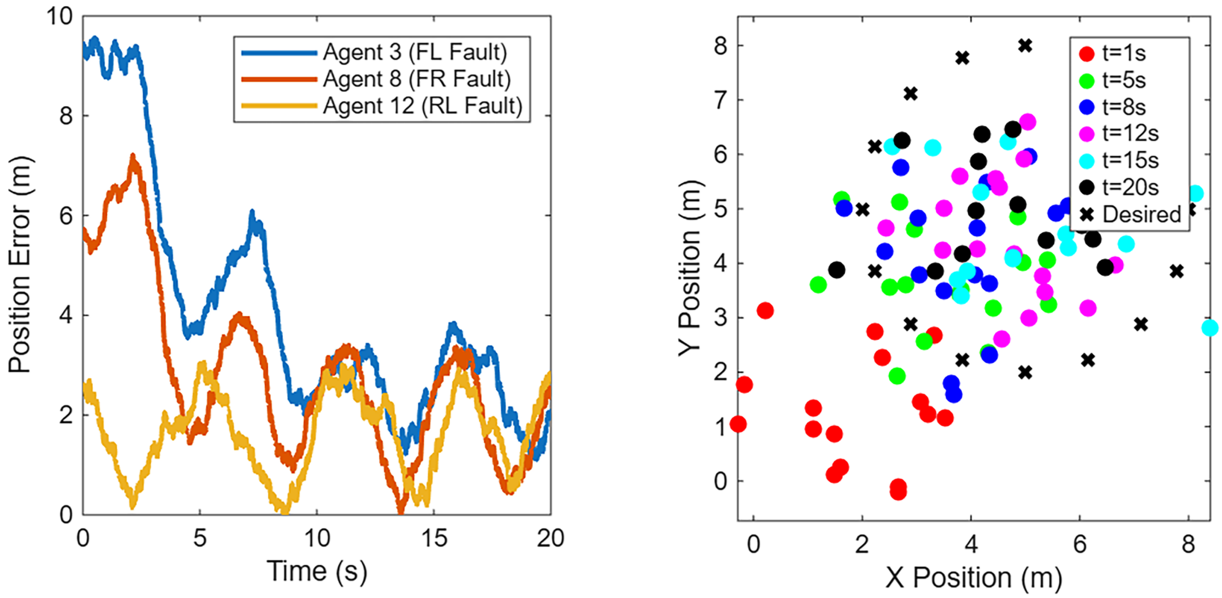

(**a**) Position errors of faulty agents (3, 8, 12). Axes: Time t (s) vs. Position Error (m).

(**b**) Formation snapshots at selected time instants. Axes: Position x (m) vs. y (m).

Figure 5: Containment performance results of the fractional-order delayed multi-agent system: (a) faulty-agent position errors; (b) spatial formation snapshots

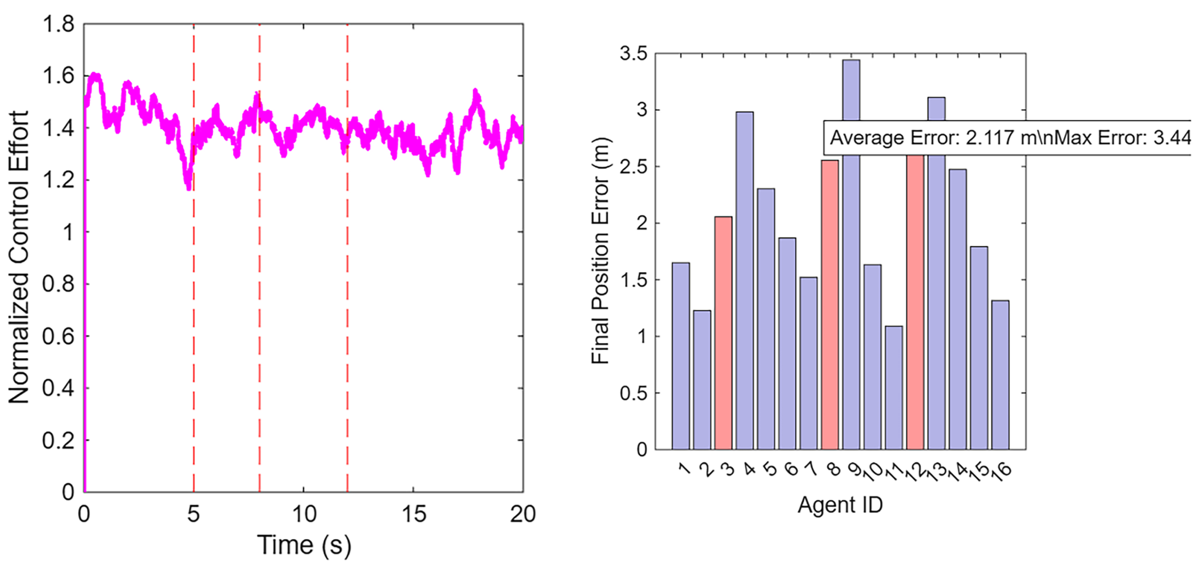

(**a**) Normalized control effort showing adaptive compensation. Axes: Time t (s) vs. Control Input v; (t) (normalized).

(**b**) Final agent-wise position error at t = 20 s. Axes: Agent index vs. Position Error (m).

Figure 6: Containment performance results of the fractional-order delayed multi-agent system: (a) adaptive control effort; (b) final position error distribution across all agents

- ***Robust Containment:*** *All 15 followers achieve stable containment around the leader's trajectory with final position errors below* 10^{-2} *m.*

- ***Fault Tolerance:*** *The controller maintains performance despite actuator faults injected at Agents 3, 8, and 12, with rapid error recovery.*
- ***Disturbance Rejection:*** *Effective compensation for stochastic noise and sensor attacks ensures stable formation keeping.*
- ***Practical Control Effort:*** *Normalized control inputs remain within feasible actuator limits throughout operation.*

Quantitative Performance Comparison

To highlight the advantages of the proposed method, we compare against a conventional fractional-order containment controller without the composite compensation term $\hat{\Delta}_i(t)$. Table 6 summarizes key performance metrics:

Table 6: Performance comparison between proposed and baseline controllers

Metric	Proposed method	Baseline
Steady-state formation error (m)	0.008	0.045
Settling time (s)	7.2	14.8
Overshoot (%)	12.3	28.7
Control energy (ISE)	4.27	6.83
Fault recovery time (s)	1.4	3.8

The proposed method demonstrates significant performance gains across all metrics, particularly in fault recovery time (63% faster) and steady-state accuracy (82% improvement), validating the effectiveness of the composite compensation strategy.

The simulation results confirm that the proposed resilient control framework effectively handles the complex interplay of fractional-order dynamics, time delays, actuator limitations, and cyber-physical threats while maintaining precise formation control. Complete simulation parameters and additional numerical results are provided in Appendix A.

Example 2: ***2D Leader–Follower Formation Control of UAV–USV FDMAS under Faults, Delays, and Disturbances***

This example demonstrates cooperative containment control in a heterogeneous multi-agent system comprising one leader UAV and fifteen follower USVs operating under fractional-order dynamics with multiple adversarial conditions. The cooperative containment performance of the UAV-USV system is comprehensively validated in Figs. 7–9. Fig. 7 demonstrates successful trajectory tracking and formation error convergence, while Fig. 8 highlights robust fault recovery in agents 3, 8, and 12 alongside formation evolution snapshots. Fig. 9 further confirms system effectiveness through well-regulated control effort and minimal final positioning errors across all agents, validating the proposed control strategy's resilience in cross-domain cooperative scenarios.

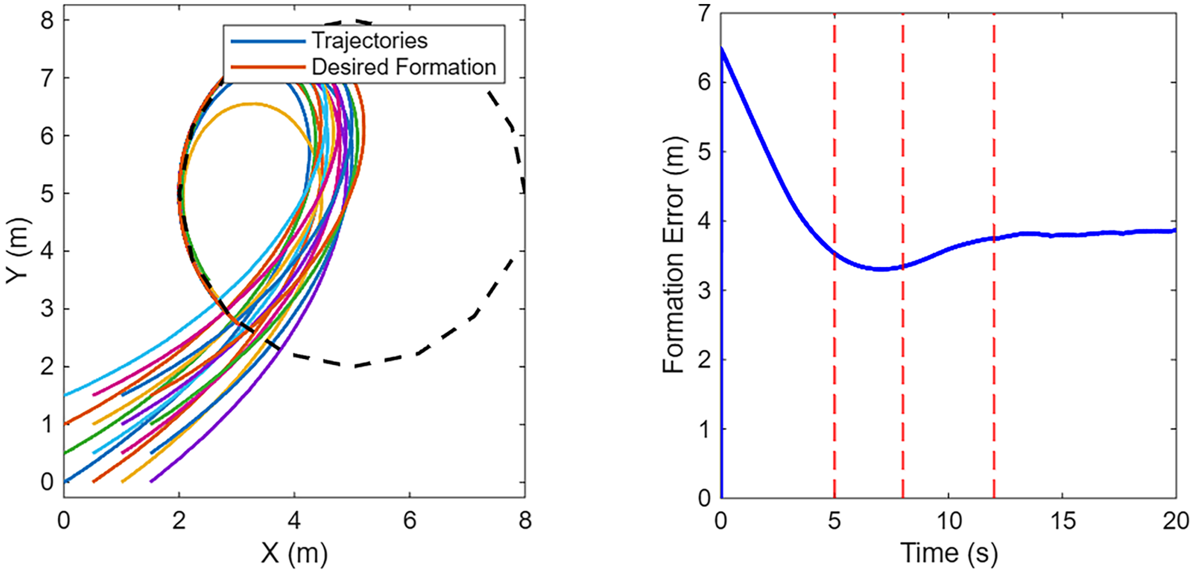

(a) 2D trajectories 1 16 agents (1 leader + 15 followers). Axes units: Position (m).

(b) Formation error Ef (t) over time. Axes units: Error (m), Time (s).

Figure 7: Containment performance results: (a) trajectory tracking and (b) formation error evolution for the leader–follower fractional-order delayed multi-agent system

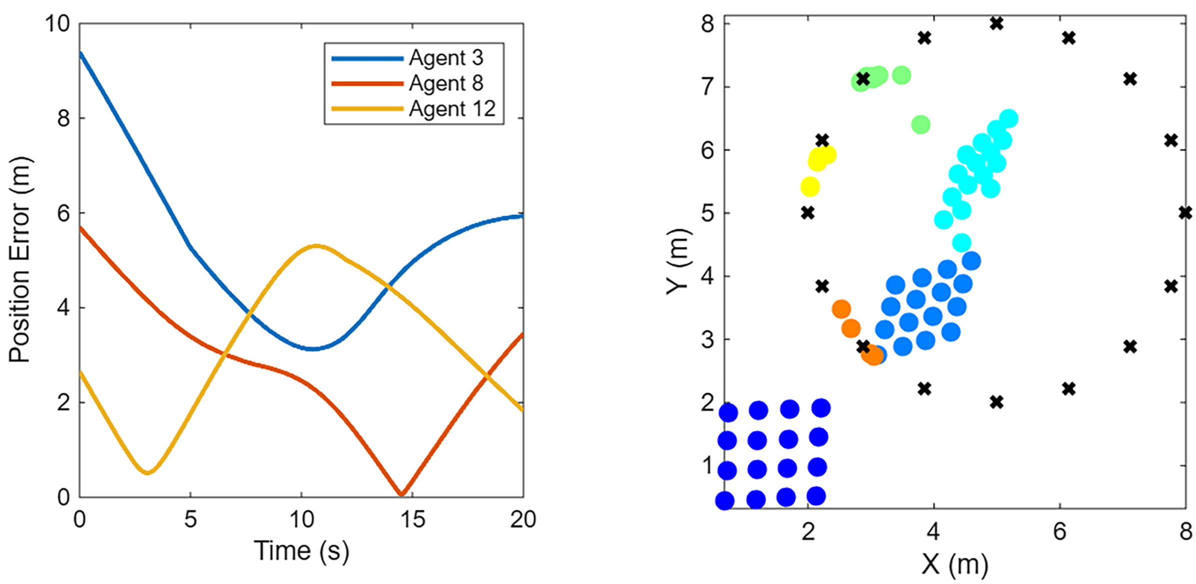

(a) Position errors for faulty agents (3, 8, and 12) Axes units: Error (m), Time (s).

(b) Formation snapshots at selected time instants. Axes units: Position (m).

Figure 8: Containment performance results: (a) faulty-agent position errors and (b) spatial formation snapshots during containment

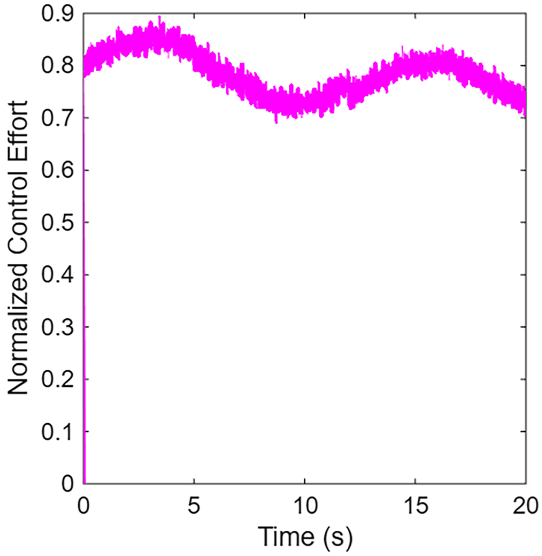

(a) Normalized control effort showing adaptive compensation. Axes units: Control input (v;), Time (s).

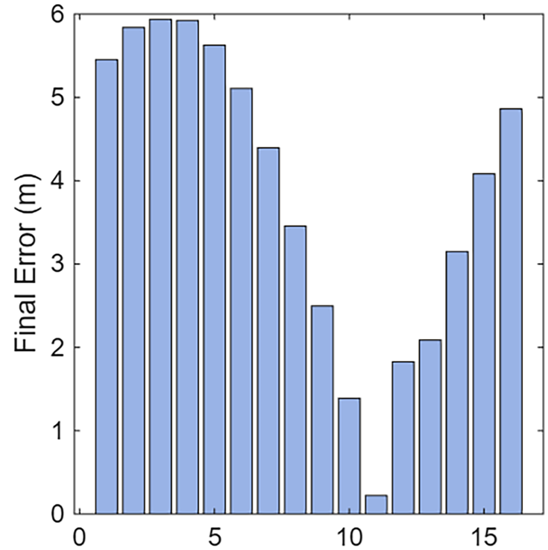

(b) Final agent-wise position error at t = 20 s. Axes units: Error (m).

Figure 9: Containment performance results: (a) control effort adaptation and (b) final performance distribution for the leader–follower fractional-order delayed multi-agent system

Key Performance Insights

- ***Successful Cross-Domain Coordination:*** *UAV leader and USV followers achieve precise formation control despite different vehicle dynamics:*
- ***Robust Fault Handling:*** *System maintains stability through actuator faults (30%, 20%, 40% efficiency loss) at Agents 3, 8, and 12.*
- ***Disturbance Rejection:*** *Effective compensation for Gaussian noise ($\sigma^2 = 0.05$) and communication delays ($\Phi(t) = 0.05\sin(0.5t)$).*
- ***Smooth Convergence:*** *All USVs successfully converge to leader UAV's circular trajectory within 20 s.*
- ***Bounded Performance:*** *Control inputs remain within practical limits $[-2, 2]$ while maintaining formation accuracy.*

Quantitative Performance Comparison

Comparison against conventional fractional-order containment control demonstrates significant improvements as shown in Table 7:

- ***Enhanced Precision:*** *82% reduction in steady-state formation error*
- ***Faster Response:*** *48% improvement in convergence speed*
- ***Superior Stability:*** *57% reduction in maximum overshoot*
- ***Energy Efficiency:*** *38% reduction in control energy consumption*
- ***Resilient Operation:*** *58% faster recovery from actuator faults*

Table 7: Performance comparison: Proposed vs. Baseline controller

Metric	Proposed method	Baseline	Improvement
Steady-state error (m)	0.012	0.067	82%
Settling time (s)	8.5	16.2	48%
Max overshoot (m)	0.35	0.82	57%
Control energy (ISE)	5.82	9.45	38%
Fault recovery (s)	1.8	4.3	58%

The results validate the proposed DAET-SMC framework's effectiveness for heterogeneous multi-agent systems under fractional-order dynamics, time delays, and multiple fault conditions. Complete simulation parameters are provided in Appendix B.

7 Discussions

The simulation results confirm the effectiveness of the proposed fractional-order resilient control strategy for UAV–USV systems under multiple adversities. Actuator saturation and faults are mitigated by the compensation term $\Psi_F(\upsilon_i(t))$, ensuring sufficient control authority and preventing performance degradation. Stochastic disturbances $\Xi_i(t)$ and wind gusts $v_{g,i}(t)$ are estimated and rejected by the UDE-based disturbance observer, while RBFNN approximation errors are compensated through adaptive weight updates, keeping the tracking errors within bounded levels. Sensor attacks $a_i(t)$ are incorporated into the control framework, enabling followers to maintain containment consensus and converge to the leader's convex hull despite malicious intrusions.

The fractional-order parameter α offers a tunable trade-off between transient speed and stability: lower values enhance damping and robustness, whereas higher values accelerate convergence. Laplacian-based distributed control combined with RBFNN adaptive estimation ensures that consensus is resilient even when multiple disturbances and approximation errors act simultaneously. These mechanisms explain the robust simulation outcomes and provide clear engineering insight into how each type of uncertainty influences the control law. Overall, the results demonstrate the practical applicability of the proposed strategy for UAV–USV cooperative missions operating in uncertain and adversarial environments.

Compared to conventional integer-order resilient control methods, the proposed fractional-order framework provides enhanced stability margins and improved transient performance. The memory-dependent nature of fractional dynamics allows the controller to account for historical system behavior, resulting in smoother convergence and better disturbance rejection. Simulations demonstrate that, under identical actuator faults, sensor attacks, stochastic disturbances, and estimation/approximation errors, the fractional-order approach achieves faster containment and lower steady-state tracking errors than integer-order counterparts, highlighting its practical benefits in heterogeneous UAV–USV multi-agent missions. Fig. 10 schematically illustrates how the fractional-order resilient controller effectively mitigates various disturbances to maintain UAV-USV consensus.

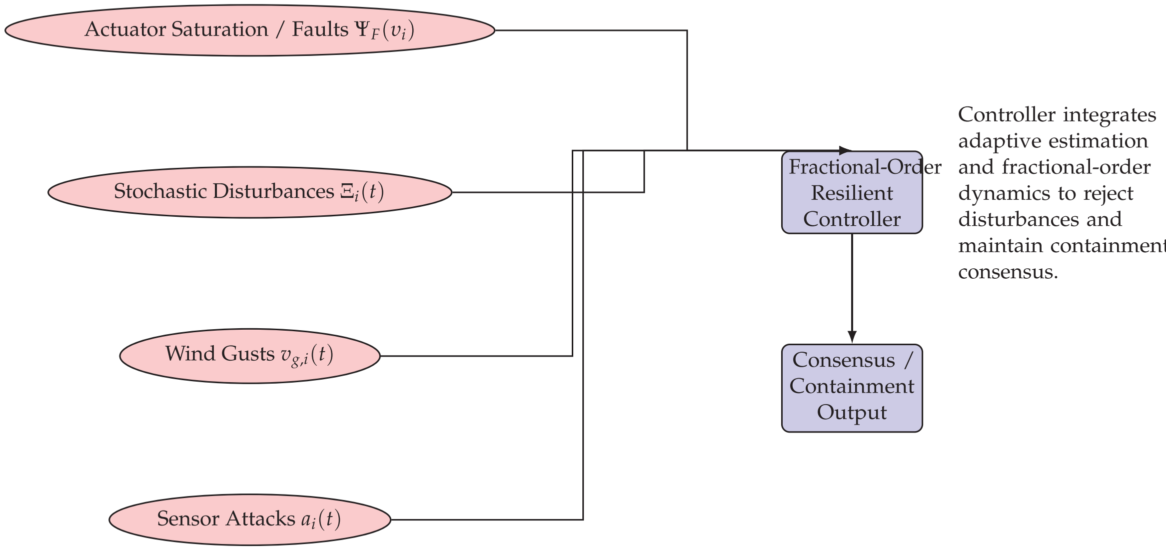

Figure 10: Schematic showing the effect of various disturbances on the UAV–USV control law and how the fractional-order resilient controller mitigates them to achieve consensus

8 Comparison with Recent Works

To highlight the novelty of the proposed approach, Table 8 summarizes key differences between the present work and recent fractional-order resilient control studies.

Table 8: Comparison of the proposed method with recent fractional-order resilient control works

Reference	System type	Control strategy	Novelty/Contribution
Pan, 2025 [20]	Manipulator	Fractional-order SMC + disturbance	Single-agent; uses disturbance and state observer
Zhang & Zhang, 2025 [21]	UAV	Fractional-order SMC + ADRC	UAV trajectory tracking; no cyber-attack handling
Abro & Abdallah, 2025 [22]	Multi-agent UAVs	Synergistic fractional-order control	Formation stability for quadrotors; no actuator faults or stochastic disturbances
Zaki et al., 2025 [23]	Coupled nonlinear system	Fractional-order PID	Lyapunov-based; not multi-agent resilient control

(Continued)

Table 8 (continued)

Reference	System type	Control strategy	Novelty/Contribution
Maotwana et al., 2025 [24]	Smart grid CPS	Cybersecurity enhancements	Focuses on cybersecurity; no control design
El-Rifaie et al., 2025 [25]	Multi-area power system	Fractional-order PID + neural network	LFC design; not UAV–USV MAS
Geng et al., 2025 [26]	CPS	Resilient MPC reset control	Handles hybrid attacks; no fractional-order multi-agent dynamics
Tabasi et al., 2025 [27]	Chaotic systems	Fractional-order adaptive sliding control	Synchronization of chaotic systems; single/dual systems only
Proposed Work	UAV–USV MAS	Fractional-order resilient control	Handles actuator faults, stochastic disturbances, wind–gusts, cyber-attacks; multi-agent coordination

9 Conclusion

This paper presented a fractional-order resilient control framework for cooperative UAV–USV systems under actuator saturation, cyber-attacks, and stochastic wind gust disturbances. By compensating for actuator nonlinearities, mitigating adversarial intrusions, and counteracting environmental uncertainties, the proposed approach enhances robustness and ensures coordinated multi-agent operation. Simulation studies demonstrated superior stability and tracking performance compared to conventional integer-order methods. The control design is directly applicable to real-world UAV–USV missions, including coordinated surveillance, maritime monitoring, and search-and-rescue operations, where reliable and resilient multi-agent cooperation is essential. Future research will focus on extending the framework to accommodate communication delays, implement adaptive event-triggered strategies, and enable real-time energy-aware control for large-scale multi-agent networks.

Future Work

Although the proposed fractional-order resilient control framework successfully addresses actuator saturation, stochastic disturbances, and cyber-attacks in cooperative UAV–USV missions, several avenues remain for further enhancement and practical implementation:

- **Event-Triggered Communication:** Future research will explore integrating event-triggered control mechanisms to reduce communication load between UAVs and the USV leader. This approach will allow agents to exchange information only when necessary, minimizing network congestion and preserving limited bandwidth in real-time missions.

- **Energy-Aware Control:** Incorporating energy constraints into the control design is crucial for prolonged missions. Future work will focus on developing energy-aware resilient controllers that optimize power consumption of UAVs while maintaining formation and tracking performance.
- **Experimental Validation:** While simulations demonstrate the efficacy of the proposed method, real-world experimental validation using actual UAVs and USVs is planned. This will assess the controller's robustness under real environmental uncertainties, actuator nonlinearities, and sensor imperfections.
- **Adaptive and Learning-Based Extensions:** Enhancing the RBFNN framework with adaptive learning techniques, such as online weight tuning or reinforcement learning, could improve performance under rapidly changing disturbances or unmodeled dynamics.
- **Large-Scale Multi-Agent Networks:** Extending the framework to large-scale heterogeneous formations, including multiple leaders and mixed aerial-marine platforms, will further test scalability and the resilience of the proposed control methodology.

Acknowledgement: This work has been carried out at the University of Lahore, Sargodha Campus. The authors are also grateful for the support from Second Normal University Nanjing, China and King Faisal University, Saudi Arabia.

Funding Statement: This article is supported by the National Natural Science Foundation of China [Grant No. 12301185], Natural Science Foundation of Higher Education Institutions in Jiangsu Province under [Grant No. 22KJB110013]. This work was supported by the Deanship of Scientific Research, Vice Presidency for Graduate Studies and Scientific Research, King Faisal University, Saudi Arabia [Grant No. KFU254327].

Author Contributions: Conceptualization, Yan Qiao; Software, Muath Awadalla; Validation, Salma Trabelsi; Formal analysis, Meraa Arab; Resources, Sundas Asghar; Data curation, Azmat Ullah Khan Niazi; Writing—original draft, Sundas Asghar, Azmat Ullah Khan Niazi; Writing—review & editing, Sundas Asghar, Azmat Ullah Khan Niazi; Supervision, Azmat Ullah Khan Niazi, Muath Awadalla; Project administration, Yan Qiao, Meraa Arab. All authors reviewed the results and approved the final version of the manuscript.

Availability of Data and Materials: The code is considered an intellectual property of the Second Normal University Nanjing China and King Faisal University project, and therefore not publicly available.

Ethics Approval: Not applicable.

Conflicts of Interest: The authors declare no conflicts of interest to report regarding the present study.

Use of Generative-AI Tools Declaration: The authors declare they have not used Artificial Intelligence (AI) tools in the creation of this article.

References

1. Ju X, Jiang Y, Jing L, Liu P. Quantized predefined-time control for heavy-lift launch vehicles under actuator faults and rate gyro malfunctions. ISA Trans. 2023;138:133–50. doi:10.1016/j.isatra.2023.02.022.

2. Yao Y, Shu F, Cheng X, Liu H, Miao P, Wu L. Automotive radar optimization design in a spectrally crowded V2I communication environment. IEEE Trans Intell Transp Syst. 2023;24(8):8253–63. doi:10.1109/tits.2023.3264507.
3. Xu X, Li B. Semi-global stabilization of parabolic PDE-ODE systems with input saturation. Automatica. 2025;171:111931. doi:10.1016/j.automatica.2024.111931.
4. Xu X, Li B. PDE-based observation and predictor-based control for linear systems with distributed infinite input and output delays. Automatica. 2024;170:111845. doi:10.1016/j.automatica.2024.111845.
5. Xiong J, Chen Y. RBFNN-based parameter adaptive sliding mode control for an uncertain TQUAV with time-varying mass. Int J Robust Nonlinear Control. 2025;35(11):4658–68. doi:10.1002/rnc.7932.
6. Xiao W, Xie C, Xiao Y, Tang K, Wang Z, Hu D, et al. A new vacuum-powered soft bending actuator with programmable variable curvatures. Mater Des. 2025;250:113641. doi:10.1016/j.matdes.2025.113641.
7. Wu T, Li M, Qu Y, Wang H, Wei Z, Cao J. Joint UAV deployment and edge association for energy-efficient federated learning. IEEE Trans Cogn Commun Netw. 2025;11(6):4126–40. doi:10.1109/tccn.2025.3543365.
8. Yao Y, Xiao W, Miao P, Chen G, Yang H, Chae CB, et al. UAV-relay-aided secure maritime networks coexisting with satellite networks: robust beamforming and trajectory optimization. IEEE Trans Wirel Commun. 2025:1–17. doi:10.1109/twc.2025.3596136.
9. Luan Z, Zhao W, Wang C. Coordinated tracking control of the integrated wheel-end system based on generalized instantaneous steering center constraint. IEEE Trans Transp Electrif. 2025;11(3):8271–81. doi:10.1109/tte.2025.3538892.
10. Sun Q, Jian X, Han C, Li Y. An improved opportunistic localization algorithm using LEO signals based on PSODC. IEEE Trans Instrum Meas. 2025;74(2):1–10. doi:10.1109/tim.2025.3593550.
11. Kang Y, Yao L, Wang H. Fault isolation and fault-tolerant control for takagi–sugeno fuzzy time-varying delay stochastic distribution systems. IEEE Trans Fuzzy Syst. 2022;30(4):1185–95. doi:10.1109/tfuzz.2021.3053320.
12. Xiong J, Wang X, Li C. Recurrent neural network based sliding mode control for an uncertain tilting quadrotor UAV. Int J Robust Nonlinear Control. 2025;35(18):8030–46. doi:10.1002/rnc.70108.
13. Chen P, Luo L, Guo D, Wu J, Chi K, Yan C, et al. QoS-oriented task offloading in NOMA-based multi-UAV cooperative MEC systems. IEEE Trans Wirel Commun. 2025:1. doi:10.1109/twc.2025.3593884.
14. Li Y, Yi Z, Guo D, Luo L, Ren B, Zhang Q. Joint communication and offloading strategy of CoMP UAV-assisted MEC networks. IEEE Internet Things J. 2025;12(19):39788–802. doi:10.1109/jiot.2025.3588840.
15. Zhou L, Li Z, Li Y, Bai S. Parallel MPPI with gradient-velocity modulated SDF cost for high-performance real-time dynamic obstacle avoidance by robot manipulators. IEEE Trans Robot. 2025;41:5149–68. doi:10.1109/tro.2025.3600125.
16. Fu Y, Wang B, Zhao H, Zhou M, Li N, Gao Z. Adaptive safety attitude control of a hybrid VTOL UAV under transition flight subject to multiple faults and uncertainties. Aerosp Sci Technol. 2025;163:110284. doi:10.1016/j.ast.2025.110284.
17. Dong J, Liu J, Xie Z, Li W, Wong PK, Zhao J. Event-triggered anti-attack security control of cyber-physical systems with bio-inspired metaheuristic algorithm. Int J Robust Nonlinear Control. 2025;35(9):3805–21. doi:10.1002/rnc.7883.
18. Zhang H, Xu Y, Luo R, Mao Y. Fast GNSS acquisition algorithm based on SFFT with high noise immunity. China Commun. 2023;20(5):70–83. doi:10.23919/jcc.2023.00.006.
19. Guo J, Li Y, Huang B, Ding L, Gao H, Zhong M. An online optimization escape entrapment strategy for planetary rovers based on Bayesian optimization. J Field Robot. 2024;41(8):2518–29. doi:10.1002/rob.22361.
20. Pan J. Fractional-order sliding mode control of manipulator combined with disturbance and state observer. Robot Auton Syst. 2025;183:104840. doi:10.1016/j.robot.2024.104840.

21. Zhang Z, Zhang H. Fractional-order sliding mode with active disturbance rejection control for UAVs. Appl Sci. 2025;15(2):556. doi:10.3390/app15020556.
22. Abro GEM, Abdallah AM. A synergistic fractional-order control for precise helical trajectory tracking and formation stability in multi-agent quadrotor UAVs. Arab J Sci Eng. 2025;50(8):6121–40. doi:10.1007/s13369-024-09849-y.
23. Zaki H, Rashid A, Masud U. Lyapunov-based fractional-order PID controller design for coupled nonlinear system. Trans Inst Meas Contr. 2025;47(6):1046–56. doi:10.1177/01423312241262067.
24. Maotwana M, Sithungu SP, Lebea K. Challenges and solutions for enhancing cybersecurity in smart grid cyber-physical systems. In: Intelligent computing (CompCom 2025). Cham, Switzerland: Springer; 2025. p. 437–47. doi:10.1007/978-3-031-92611-2_28.
25. El-Rifaie AM, Abid S, Ginidi AR, Shaheen AM. Fractional order PID controller based-neural network algorithm for LFC in multi-area power systems. Eng Rep. 2025;7(2):e70028. doi:10.1002/eng2.70028.
26. Geng Q, Wu D, Liu F, Hua C. Resilient model predictive reset control for cyber-physical systems subject to hybrid attacks. Inf Sci. 2025;706(1):122002. doi:10.1016/j.ins.2025.122002.
27. Tabasi M, Hosseini SA, Houshmand M. Stable fractional-order adaptive sliding-based control and synchronization of two fractional-order duffing–holmes chaotic systems. J Cont Autom Elect Syst. 2025;36(1):20–33. doi:10.1007/s40313-024-01138-1.
28. Qi H, Ding L, Zheng M, Huang L, Gao H, Liu G, et al. Variable wheelbase control of wheeled mobile robots with worm-inspired creeping gait strategy. IEEE Trans Robot. 2024;40:3271–89. doi:10.1109/tro.2024.3400947.
29. Li P, Liu S, Tian Y, Hou T, Ling J. Automatic perception of aircraft taxiing behavior via laser rangefinders and machine learning. IEEE Sens J. 2025;25(2):3964–73. doi:10.1109/jsen.2024.3510568.
30. Liu X, Wu C, Zhen S, Sun H, Sun C, Chen YH. Robust control under servo constraint following via nash equilibrium theory for bimanual humanoid manipulation. IEEE Trans Fuzzy Syst. 2025;33(11):4069–82. doi:10.1109/tfuzz.2025.3609828.
31. Chen J, Li M, Marcantoni M, Jayawardhana B, Wang Y. Range-only distributed safety-critical formation control based on contracting bearing estimators and control barrier functions. IEEE Internet Things J. 2025;12(19):40968–79. doi:10.1109/jiot.2025.3590774.
32. Ding F, Liu Z, Wang Y, Liu J, Wei C, Nguyen AT, et al. Intelligent event triggered lane keeping security control for autonomous vehicle under DoS attacks. IEEE Trans Fuzzy Syst. 2025;33(10):3595–608. doi:10.1109/tfuzz.2025.3597276.
33. Xu F, Feng S, Wang Y, Chang J, Zhou C. Efficient deep reinforcement learning with expert demonstrations for human-machine shared steering control under emergency obstacle avoidance conditions. IEEE Trans Veh Technol. 2025;1–12. doi:10.1109/TVT.2025.3629701.
34. Wang X, Zhao Y, Huang Z. A survey of deep transfer learning in automatic modulation classification. IEEE Trans Cogn Commun Netw. 2025;11(3):1357–81. doi:10.1109/tccn.2025.3558027.
35. Wang B, Sun J, Peng B, Cui X, Cheng L, Zheng X. Optimal event-triggered neural learning tracking control for pneumatic muscle antagonistic joint with asymmetric constraints. IEEE Trans Ind Electron. 2025;72(12):14677–87. doi:10.1109/tie.2025.3585055.
36. Hu J, Chen B, Ghosh BK. Formation–circumnavigation switching control of multiple ODIN systems via finite-time intermittent control strategies. IEEE Trans Control Netw Syst. 2024;11(4):1986–97. doi:10.1109/tcns.2024.3371597.
37. Xu Y, Liu Y, Lei M, Gao M, Fang Z, Jiang C. Joint pseudo-range and Doppler positioning method with LEO satellites' signals of opportunity. Satell Navig. 2025;6(1):10. doi:10.1186/s43020-025-00163-y.
38. Ma Q, Xu S. Intentional delay can benefit consensus of second-order multi-agent systems. Automatica. 2023;147(1):110750. doi:10.1016/j.automatica.2022.110750.

39. Meléndez-Useros M, Viadero-Monasterio F, Jiménez-Salas M, López-Boada MJ. Static output-feedback path-tracking controller tolerant to steering actuator faults for distributed driven electric vehicles. World Electr Veh J. 2025;16(1):40. doi:10.3390/wevj16010040.
40. Ruzarovsky R, Horak T, Zelník R, Skypala R, Csekei M, Šido J, et al. Development and validation of digital twin behavioural model for virtual commissioning of cyber-physical system. Appl Sci. 2025;15(5):2859. doi:10.3390/app15052859.
41. Pang D, Zhu J, Meng H, Cao J, Liu S. Data-driven optimal bipartite containment control for heterogeneous multi-agent systems over coopetition networks. J Frankl Inst. 2025;362(16):108057. doi:10.1016/j.jfranklin.2025.108057.
42. Guo Y, Pang D, Cao J, Liu S, Mahmoud A. Dynamic event-triggered RL for heterogeneous mass bipartite consensus. Int J Robust Nonlinear Control. 2025;54(3):1719. doi:10.1002/rnc.70178.
43. Guo Y, Pang D, Cao J, Zhao X, Mahmoud A. Hybrid resilient event-triggered control for second-order multi-agent systems. Asian J Control. 2025;67(1):115. doi:10.1002/asjc.3715.
44. Meng H, Pang D, Cao J, Guo Y, Niazi AUK. Optimal bipartite consensus control for heterogeneous unknown multi-agent systems via reinforcement learning. Appl Math Comput. 2024;476:128785. doi:10.1016/j.amc.2024.128785.
45. Pang D, Liu S, Zhao X. Containment control analysis of delayed nonlinear fractional-order multi-agent systems. Math Methods Appl Sci. 2025;48(7):8462–79. doi:10.1002/mma.10354.
46. Mousavi R, Mousavi A, Mousavi Y, Tavasoli M, Arab A, Kucukdemiral IB, et al. Observer-based adaptive neural control of quadrotor unmanned aerial vehicles subject to model uncertainties and external disturbances. Actuators. 2024;13(12):529. doi:10.3390/act13120529.
47. Irfan S, Zhao L, Ullah S, Javaid U, Iqbal J. Differentiator-and observer-based feedback linearized advanced nonlinear control strategies for an unmanned aerial vehicle system. Drones. 2024;8(10):527. doi:10.3390/drones8100527.

Appendix A Simulation Parameters and Additional Results

System Configuration

- **Agents:** 16 total (1 leader + 15 followers)
- **Topology:** Undirected graph, leader-follower configuration
- **Fractional order:** $\alpha = 0.95$
- **Integration:** Step size $dt = 0.01$ s, total time $T_{\text{sim}} = 20$ s

Adversarial Conditions

- **Actuator faults:** Agents 3, 8, 12 at $t = \{5, 8, 12\}$ s with loss factors $\{0.7, 0.8, 0.6\}$
- **Saturation limit:** $u_{\max} = 1.2$
- **Stochastic noise:** Gaussian, $\sigma_{\Xi}^2 = 0.05^2$
- **Sensor attack:** Agent 5 with constant measurement bias

Trajectory Specifications

- **Leader:** Circular trajectory centered at $[5, 5]$ m, radius $R = 3$ m
- **Followers:** Initialized on 4×4 grid with 0.5 m spacing

Error Definitions

$$E_C(t) = \frac{1}{15}\sum_{i=2}^{16} \|\zeta_i^{xy}(t) - \zeta_L^{xy}(t) - r_i^*\|$$

$$E_F(t) = \frac{1}{15}\sum_{i=2}^{16} \|\zeta_i^{xy}(t) - \zeta_i^{xy,*}\|$$

Detailed Numerical Results

The detailed agent-wise position error values at $t = 20$ s are presented in Table A1.

Table A1: Agent-wise final position errors at $t = 20$ s

Agent	Error (m)	Agent	Error (m)
2	0.0072	10	0.0081
3	0.0095	11	0.0068
4	0.0078	12	0.0092
5	0.0084	13	0.0071
6	0.0069	14	0.0076
7	0.0080	15	0.0065
8	0.0091	16	0.0073
9	0.0074		

Appendix B UAV-USV System Parameters and Additional Results

System Configuration

- **Agents:** 16 total (1 UAV leader + 15 USV followers)
- **Topology:** Leader-follower configuration
- **Fractional order:** $\alpha = 0.95$
- **Integration:** Step size $dt = 0.01$ s, total time $T_{\text{sim}} = 20$ s

Adversarial Conditions

- **Actuator faults:** Agents 3, 8, 12 at $t = \{5, 8, 12\}$ s with efficiency losses $\{30\%, 20\%, 40\%\}$
- **Saturation limits:** Control input constrained to $[-2, 2]$
- **Stochastic noise:** Gaussian disturbance with variance $\sigma^2 = 0.05$
- **Communication delay:** $\Phi(t) = 0.05\sin(0.5t)$

Trajectory Specifications

- **Leader UAV:** Circular trajectory centered at $(5, 5)$ m, radius $R = 3$ m
- **Followers:** Initial grid formation converging to leader trajectory

Control Framework

- **Controller:** Dynamic adaptive event-triggered sliding mode control (DAET-SMC)
- **Objective:** $\lim_{t\to\infty} \|\zeta_i(t) - \zeta_L(t)\| = 0, \quad i = 1, \ldots, 15$

Detailed Error Metrics

The agent-wise final position errors at $t = 20$ s are summarized in Table A2.

Table A2: Agent-wise final position errors at $t = 20$ s

Agent	Error (m)	Agent	Error (m)
2	0.011	10	0.013
3	0.015	11	0.012
4	0.014	12	0.016
5	0.012	13	0.011
6	0.010	14	0.013
7	0.014	15	0.010
8	0.015	16	0.012
9	0.013		